First results from H-mode plasmas generated by ICRF heating in the EAST

2013 Nucl. Fusion 53 023004

(http://iopscience.iop.org/0029-5515/53/2/023004)

IOP PUBLISHING and INTERNATIONAL ATOMIC ENERGY AGENCY NUCLEAR FUSION
Nucl. Fusion **53** (2013) 023004 (6pp) doi:10.1088/0029-5515/53/2/023004

First results from H-mode plasmas generated by ICRF heating in the EAST

X.J. Zhang[1], Y.P. Zhao[1], B.N. Wan[1], X.Z. Gong[1], J.G. Li[1], Y. Lin[2], C.M. Qin[1], G. Taylor[3], G.S. Xu[1], Y.W. Sun[1], B.X. Gao[4], J.P. Qian[1], F.D. Wang[1], B. Lu[1], C. Luo[4], L. Zhang[1], L.Q. Hu[1], Y.T. Song[1], C.X. Yu[4], W.D. Liu[4], S Wukitch[2], J.R. Wilson[3] and J.C. Hosea[3]

[1] Institute of Plasma Physics, Chinese Academy of Sciences, Hefei 230031, People's Republic of China
[2] MIT Plasma Science and Fusion Center, Cambridge, MA 02139, USA
[3] Princeton Plasma Physics Laboratory, Princeton, NJ 08543, USA
[4] CAS Key Laboratory of Basic Plasma Physics, Department of Modern Physics, University of Science and Technology of China, Hefei, Anhui 230026, People's Republic of China

E-mail: xjzhang@ipp.ac.cn

Received 16 September 2012, accepted for publication 31 December 2012
Published 28 January 2013
Online at stacks.iop.org/NF/53/023004

Abstract
Deuterium high-confinement (H-mode) plasmas, lasting up to 3.45 s, have been generated in the EAST by ion cyclotron range of frequency (ICRF) heating. H-mode access was achieved by coating the molybdenum-tiled first wall with lithium to reduce the hydrogen recycling from the wall. H-mode plasmas with plasma currents between 0.4 and 0.6 MA and axial toroidal magnetic fields between 1.85 and 1.95 T were generated by 27 MHz ICRF heating of deuterium plasma with hydrogen minority. The ICRF input power required to access the H-mode was 1.6–1.8 MW. The line-averaged density was in the range (1.83–2.3) $\times 10^{19}\,\mathrm{m}^{-3}$. 200–500 Hz type-III edge localized mode activity was observed during the H-mode phase. The H-mode confinement factor, $H_{98\mathrm{IPB}}(y, 2)$, was ∼0.7.

(Some figures may appear in colour only in the online journal)

1. Introduction

The high-confinement or 'H-mode' of operation was first discovered in the Asymmeteric Divertor Experiment (ASDEX) when deuterium plasmas were heated by neutral beam injection [1]. Later, on the same machine, H-mode plasmas were generated in a deuterium plasma with a hydrogen minority with ion cyclotron range of frequency (ICRF) minority heating [2]. H-mode plasmas have since been observed in many other tokomaks [3–6]. This paper presents results for the first H-mode plasmas produced by using ICRF heating as the only auxiliary power source in the Experimental Advanced Superconducting Tokamak (EAST) [7]. These experiments were performed with a molybdenum first-wall and all of these results have been obtained with lithium wall conditioning [8, 9], which reduced hydrogen recycling from the wall. As a result, the hydrogen concentration was reduced to as low as 5% in the plasma and the ICRF power absorption was improved [10–12]. The ICRH H-mode plasmas in EAST were characterized by an ICRF power deposition profile that was strongly peaked on the magnetic axis and the low-confinement (L-mode) to H-mode threshold power was close to the value predicted by the international tokamak scaling [13]. The ICRH H-modes were also exhibited by rapid type-III edge localized mode (ELM) activity and had H-mode confinement factor, $H_{98\mathrm{IPB}}(y, 2)$, of ∼0.7.

2. Experimental setup

EAST is a superconducting tokamak with toroidal divertor configuration [7] ($R_0 = 1.88$ m, $a = 0.45$ m, $B_0 < 3.5$ T, $I_p \sim 1$ MA), which commenced operation in September 2006. EAST was designed for steady-state divertor operation for a duration of 1000 s and has achieved 410 s to date. ICRF heating is the sole auxiliary heating method used in these discharges. Fundamental hydrogen (H)-minority heating at 27 MHz with the power available (up to 1.8 MW) is used for central heating of deuterium (D) majority plasmas for ICRF heated H-mode studies. An example of a typical EAST equilibrium shape at typical magnetic field $B_0 \sim 1.95$ T is shown in figure 1.

The available source power of the ICRF system in the 2012 experimental campaign was 6.0 MW with two dedicated horizontal ports, at B-port and I-port. The ICRF antenna at

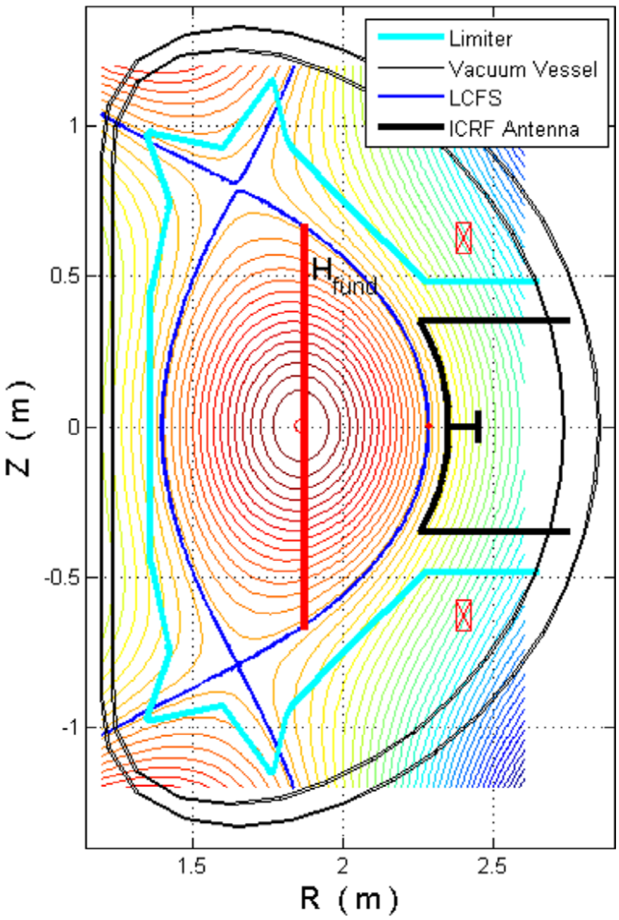

Figure 1. Double null magnetic flux contour from a typical H-mode discharge in EAST ($I_p = 0.5$ MA and $B_0 = 1.95$ T).

B-port had two straps constructed of stainless steel and coated with boron carbide (B_4C). The I-port antenna had four straps and was also constructed of stainless steel, but it was not coated.

The ICRF power deposition profile during the H-mode phase, as calculated with the 2D full wave TORIC code [14, 15], was peaked near the magnetic axis, $\rho \sim 0.1$ (as indicated by the vertical red line in figure 1). This is also confirmed by an ECE imaging (ECEI) diagnostic [16, 17], as shown in figure 2. The ECE data clearly show that the electron temperature increase during the ICRF heating pulse is peaked near the magnetic axis, at $\rho \sim 0.1$, as predicted by TORIC. For the purposes of this study, and consistent with previous reports [10], the ICRF coupling efficiency can be simply estimated by calculating dW_{dia}/dt at the time of the ICRF power turn-on.

3. Experimental results

In this campaign, 25 H-mode discharges were obtained in total. The H modes have been obtained with double null only with an elongation ~1.7, and a triangularity ~0.45. The H-mode plasmas with ICRF heating alone have been produced in a narrow range of operation parameters with plasma currents of $0.4\,\text{MA} < I_P < 0.6\,\text{MA}$, line-averaged density from $1.83 \times 10^{19}\,\text{m}^{-3}$ to $2.35 \times 10^{19}\,\text{m}^{-3}$, $B_0 = 1.85 - 1.95$ T. The total input power for ICRF H-mode plasmas in this campaign has varied from 1.6 to 1.8 MW. Note that a higher plasma density is needed for effective coupling of ICRF power into the core plasma. Normally, arcing was encountered in the RF transmission line when the line-averaged plasma density was less than $1.8 \times 10^{19}\,\text{m}^{-3}$. This was due to increased reflection of RF power back into the antennas causing standing waves in the transmission line.

ELMing ICRF heated H-mode discharges were generated in EAST with durations of up to 3.45 s, as shown in figures 3 and 4. Figure 3 shows a discharge that had a total ICRF power of 1.7 MW (figure 3(*g*)). The pre-transition plasma density is about $2.0 \times 10^{19}\,\text{m}^{-3}$ (figure 3(*b*)). Transition from L-mode to H-mode takes place after a sudden drop of D_α emission (as indicated in figure 4(*a*)) and a successive increase in stored energy and electron density. Plasma density and stored energy more than doubled during the H-mode phase (figures 4(*b*) and (*d*)). Confirmation of pedestal formation during the H-mode phase came from the density profiles (figure 3(*b*)) and the extreme ultra-violet (XUV) radiation (figure 3(*f*)). The density profiles from the microwave reflectometry clearly demonstrated pedestal formation at the onset of H-mode. This was further confirmed by a sharp rise in the XUV radiation at the plasma edge ($\rho = 0.9$) as shown in figure 3(*f*). Unlike EAST H-mode discharges generated by lower hybrid wave (LHW) heating alone, which exhibit a decrease of the core electron temperature, the electron temperature (see in figure 5(*a*)) measured by an x-ray crystal spectrometer (XCS) [18] showed an increase of 300 eV in the plasma core of a H-mode discharge heated only by ICRF power, even though the enhanced density and radiation power loss during the H-mode phase were greatly enhanced. The increase in the ion temperature and the toroidal rotation at the plasma centre are about 300 eV and 20 km s^{-1}, respectively. As shown in figure 4, H-modes started with a short ELM-free period, lasting ~500 ms, followed by type-III ELMs (figure 4(*a*)) with frequencies from 200 to 500 Hz (figure 4(*b*)). Confinement times for the H-mode discharges (with type-III ELMs) are in the range 110–150 ms for 1.7 MW of total heating power at 500 kA. The H factor, $H_{IPB98(y,2)}$, for the L-mode plasma just before the transitions is about 0.5 and then up to 0.7 ± 0.1.

4. Access to H-mode

To assess the operating parameters needed to access the H-mode regime, the toroidal field and plasma density were scanned during a sequence of deuterium discharges that had the same plasma shape and a plasma current of 500 kA. All of the discharges had a lithium coated first-wall and a double null plasma configuration. Figure 6 shows the H-mode operational window in plots of injected ICRF power versus plasma density and toroidal magnetic field. For the plasma density scan, the magnetic field was fixed at 1.95 T at a constant target plasma current of 500 kA for on-axis heating. The density was scanned from shot-to-shot from low densities up to a level where a H-mode was no longer achievable with the ICRF power available (~1.8 MW). Figure 6(*a*) shows that it was possible to access the H-mode regime when the plasma density was less than $2.35 \times 10^{19}\,\text{m}^{-3}$. Figure 6(*b*) shows that it was possible to access the H-mode regime when the axial toroidal field was between 1.85 and 1.95 T. It is clear from this parameter

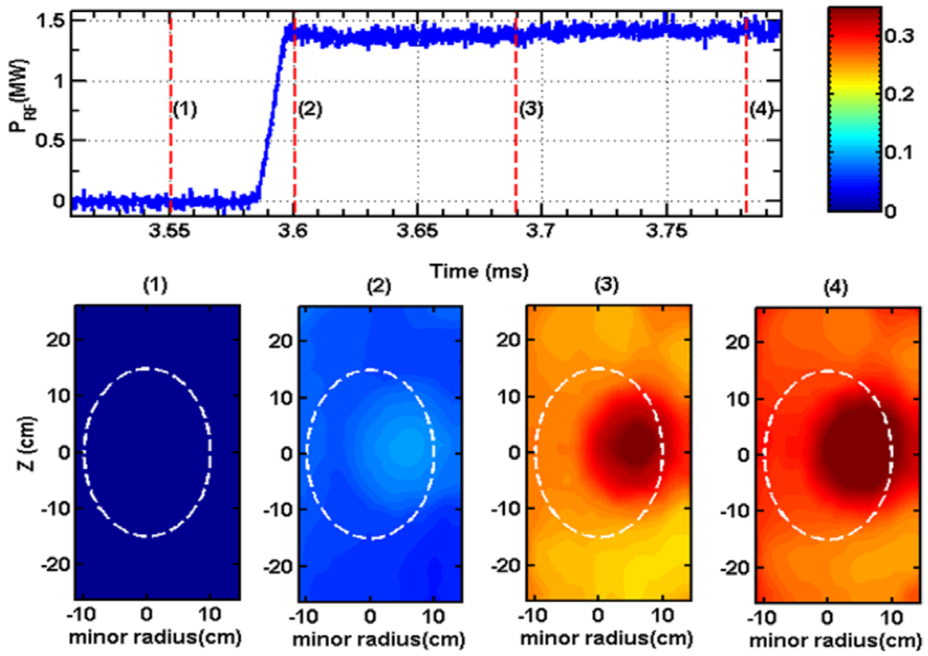

Figure 2. The 2D image of the temperature change measured by the ECEI diagnostic (here, we define $\Delta T_e = (T_e - T_{e0})/T_{e0}$) during the ICRF heating pulse; the white dashed ellipses in figure 2 represent the $q = 1$ surface.

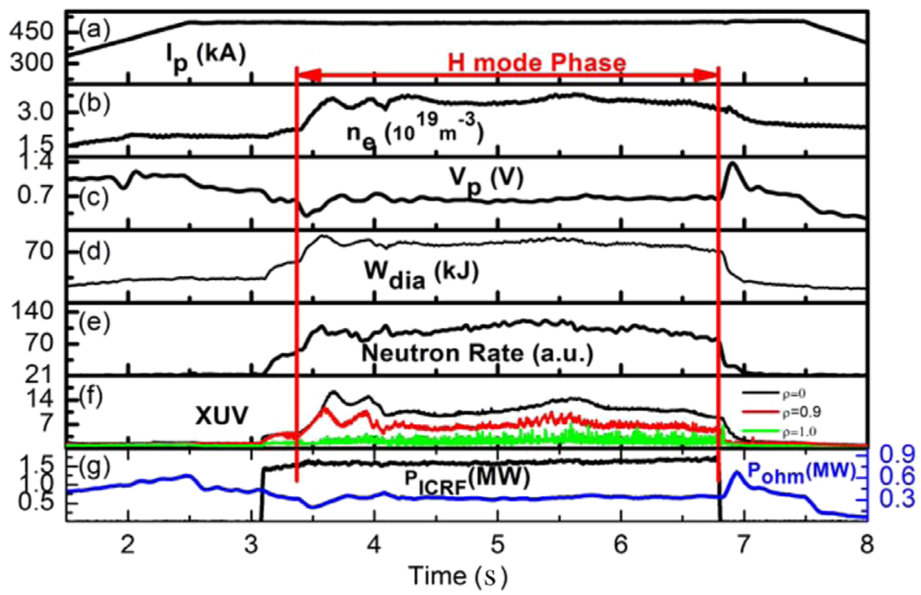

Figure 3. Time traces of plasma parameters for typical H-mode discharges with ICRH only: (*a*) plasma current; (*b*) the line-averaged density; (*c*) the loop voltage; (*d*) the stored energy; (*e*) the neutron rate; (*f*) XUV radiations at $\rho = 0$, 0.9 and 1; (*g*) ICRF injection power. The plasma is in the H-mode starting at 3.4 s and is sustained in H-mode up to 6.85 s.

scan that much higher ICRF power needs to be coupled into the plasma in order to generate H-mode discharges that are resilient to significant changes in plasma density and toroidal magnetic field.

5. Power threshold

In the 2010 autumn campaign of EAST [19], a H-mode with type-III ELMs at a H factor of $H_{98IPB}(y, 2) = 0.8 \pm 0.2$ was produced by LHW as the only auxiliary power source with strongly off-axis power deposition at a power level close to 1 MW. A threshold in density for H-mode access was identified, $\bar{n}_e > 1.9 \times 10^{19}\,m^{-3}$. It is widely known that the transition from L-mode to H-mode is obtained when the input power exceeds a threshold (P_{thresh}), which depends on the plasma density and the magnetic field. It also depends on other parameters such as the plasma shape, the neutral density or the vacuum vessel conditioning. The power threshold for H-mode access has been studied on several machines including DIIID [20], JET [21], Alcator C-Mod [22], ASDEX Upgrade [23] and JT-60U [24]. The threshold power for ITER are also discussed [25].The H-mode discharges generated by ICRF heating alone

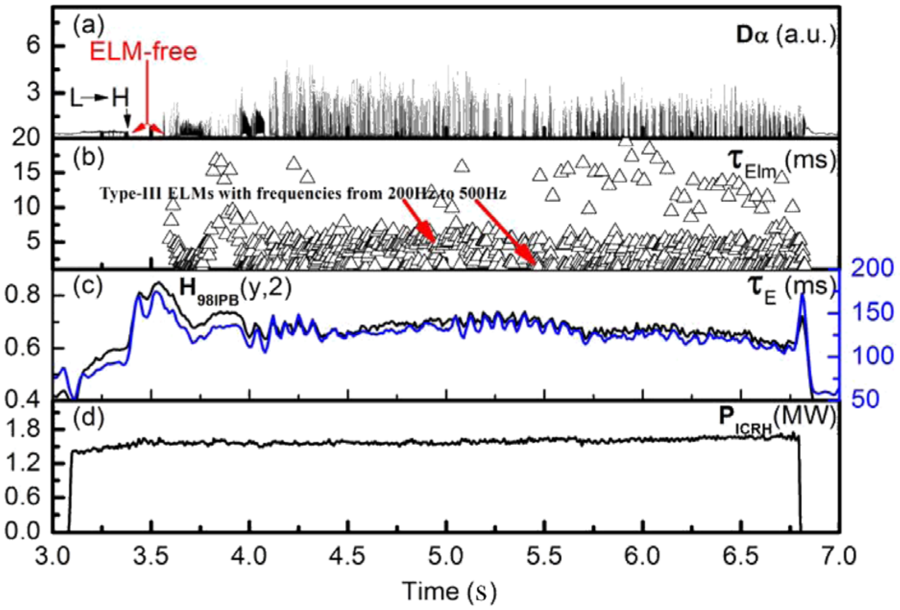

Figure 4. An expanded time scale near ICRF power: (*a*) D_α emission, (*b*) ELM repetition time and, (*c*) $H_{98yIPB}(y2)$ and τ_E, (*d*) ICRF heating power versus time during the ELMy ICRF-heated H-mode discharge type-III ELMs with frequencies between 200 and 500 Hz were observed.

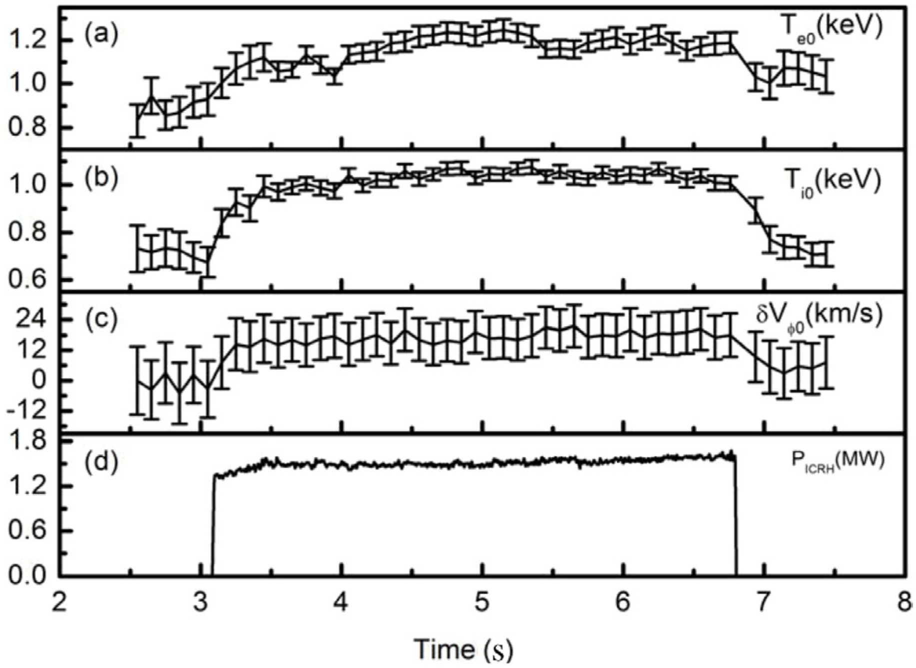

Figure 5. The data at the plasma centre were measured by XCS for the same shot as in figure 3: (*a*) the electron temperature, (*b*) the ion temperature, (*c*) the toroidal rotation, (*d*) ICRH injected power.

in EAST extend the density range down to $1.83 \times 10^{19}\,\mathrm{m}^{-3}$, as shown in figure 7(*b*).

The duration of the first ICRF H-mode discharge generated in EAST was about 500 ms because the coupled ICRF power was marginal compared to P_{thresh}, multiple L–H–L transitions were observed during a single shot as the plasma current was increased from 400 to 600 kA. H–L back transitions were attributed to increased power loss by radiation (P_{rad}). But the ICRF power coupled to the plasma stayed constant during the L–H transitions and H-mode phases. Figure 7(*a*) shows that P_{loss} at the L–H transitions is similar to the P_{thresh} predicted by the international tokomak scaling [13], showing that it follows the scaling. P_{loss} is calculated as the sum of the absorbed ICRF power and the ohmic power (P_{oh}) minus P_{rad} and the time variation of the stored energy $\mathrm{d}W_{\mathrm{dia}}/\mathrm{d}t$. In the present analysis, fast ion loss is ignored. Note that P_{rad} is subtracted to estimate P_{loss} even though P_{rad} is not especially taken into account for the evaluation of P_{loss} in the threshold power scaling study [13]. In figure 7(*b*), P_{loss} is plotted as a function of $\bar{n}_{\mathrm{e}}$. A threshold in density for H-mode access was identified, $\bar{n}_{\mathrm{e}} > 1.83 \times 10^{19}\,\mathrm{m}^{-3}$. Interestingly we can see the two routes of the density dependence of the threshold power,

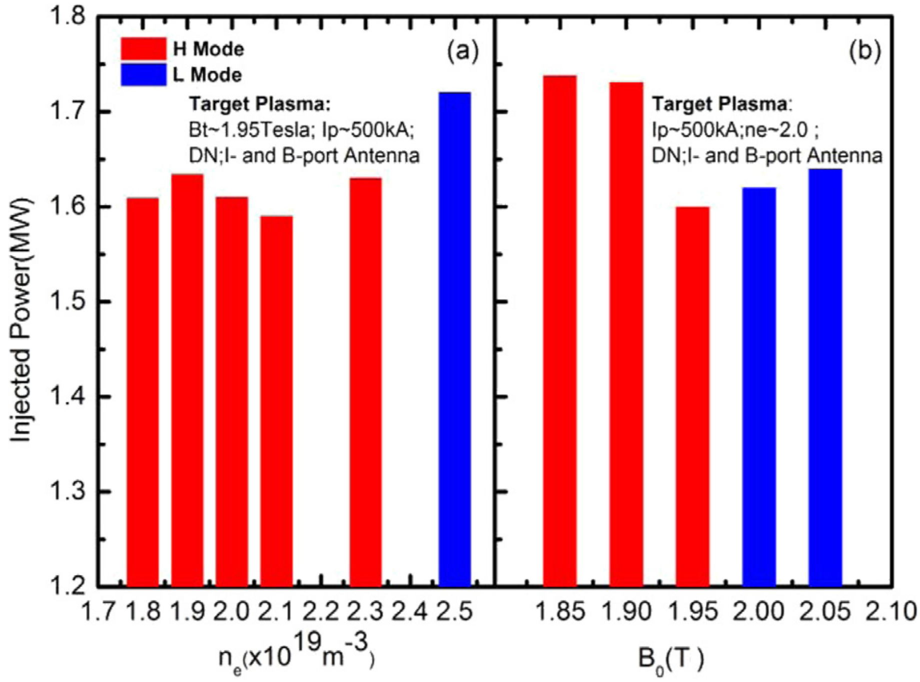

Figure 6. ICRF heated H-mode with the ICRF power available (up to 1.8 MW) in EAST: (*a*) total injected power versus the line-averaged density taken just before the first L–H transition; (*b*) total injected power versus toroidal field.

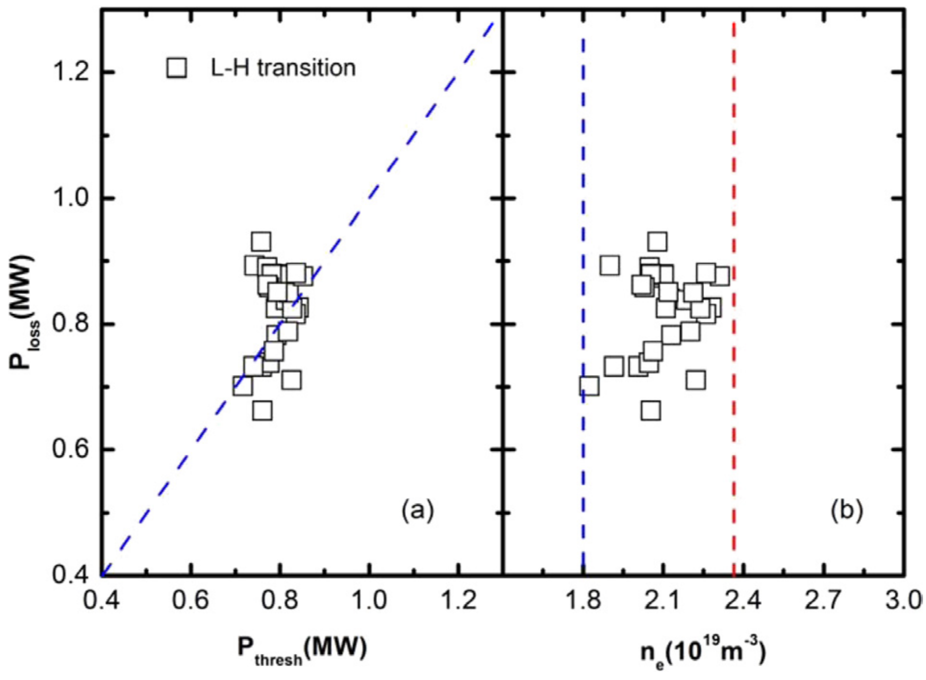

Figure 7. Loss powers ($P_{\rm loss}$) through the separatrix at L–H and H–L transitions versus the threshold powers ($P_{\rm thresh}$) predicted by the international tokamak scaling. The threshold power is expressed as $P_{\rm thresh} = 0.0488 \times n_{\rm e20}^{0.72} \times B_0^{0.80} \times S_{\rm A}^{0.94}$, where B_0 is in T, and $S_{\rm A}$ are in units of $\rm m^2$.

one is $P_{\rm loss}$ increases with $\bar{n}_{\rm e}$ and the other is $P_{\rm loss}$ increased with the decrease of $\bar{n}_{\rm e}$.

6. Summary

In summary, a sustained H-mode was demonstrated in EAST using ICRF heating alone for the first time. The discharges were characterized by 200–500 Hz type-III ELMs and a sustained enhanced confinement factor, $H_{98\rm IPB}(y, 2) \sim 0.7$. The threshold power for H-mode access follows the international tokamak scaling, even in the low density regime studied here. To access the H-mode regime with the available ICRF power (up to 1.8 MW) it was found necessary to use lithium wall conditioning to reduce the hydrogen concentration and improve the ICRF power absorption. Arcing in the transmission lines between the RF sources and the antennas was one of the main issues limiting the RF power that could be coupled into the plasma during the 2012 EAST experimental campaign. More coupled power will be required to achieve H-mode access with ICRF power alone at even lower plasma density. In future, effects of $P_{\rm rad}$ on the threshold power will be studied precisely, which would contribute to the further study whether the two routes of the density dependence of the threshold power are of the transition physics problem or of the plasma conditioning problem.

Acknowledgments

The authors would like to acknowledge the support of the EAST operation and diagnostics group. This work was supported partly by National Magnetic confinement Fusion Science Programme (grant nos 2010GB110000, 2009GB107001, 2011GB107001, 2011GB101001, 2011GB107003 and 2012GB101001). This work was also supported partly by the National Natural Science Foundation of China under grant nos 10725523, 10721505, 11105179, 10928509, 10990212, 11075182, 10975155 and 11175208. This work was supported partly by the Knowledge Innovation Programme of the Chinese Academy of Sciences no Y05FCQ0126 and JSPS-NRF-NSFC A3 Foresight Program in the field of Plasma Physics (NSFC no. 11261140328). Gary Taylor, Joel Hosea and Randy Wilson are supported at PPPL by US DoE contract no DE-AC02-09CH11466. Y. Lin and S. Wukitch are supported at MIT by US DoE contract no DE-FC02-99ER54512.

References

[1] Wagner F. *et al* 1982 *Phys. Rev. Lett.* **49** 1408
[2] ASDEX Team 1989 *Nucl. Fusion* **29** 1959
[3] Nagami M. *et al* 1984 *Nucl. Fusion* **24** 183
[4] Tanga A. 1987 *Nucl. Fusion* **27** 1877
[5] Greenwald M. *et al* 1997 *Nucl. Fusion* **37** 793
[6] Wagner F. 2007 *Plasma Phys. Control. Fusion* **49** B1
[7] Wan B. *et al* 2009 *Nucl. Fusion* **49** 104011
[8] Hu J.S. *et al* 2009 *Fusion Eng. Des.* **84** 2167
[9] Zuo G.Z. *et al* 2010 *Plasma Sci. Technol.* **12** 646
[10] Bonoli P.T. *et al* 2007 *Fusion Sci. Technol.* **51** 401
[11] Zhang X.J. *et al* 2011 *Plasma Sci. Technol.* **13** 172
[12] Zhang X.J. *et al* 2012 *Nucl. Fusion* **52** 032002
[13] Martin Y.R., Takizuka T. and ITPA CDBM H-mode Threshold Database Working Group 2008 *J. Phys.: Conf. Ser.* **123** 012033
[14] Brambilla M. 1999 *Plasma Phys. Control. Fusion* **41** 1
[15] Wright J.C. *et al* 2004 *Phys. Plasmas* **11** 2473
[16] Xu M. *et al* 2011 *Plasma Sci. Technol.* **13** 167
[17] Gao B.X. *et al* and USTC ECEI Team 2013 384 channel ECE imaging system on EAST tokamak *Rev. Sci. Instrum.* submitted
[18] Shi Y.J. *et al* 2010 *Plasma Phys. Control. Fusion* **52** 085014
[19] Xu G.S. *et al* 2011 *Nucl. Fusion* **51** 072001
[20] Burrell K.H. *et al* 1989 *Plasma Phys. Control. Fusion* **31** 1649
[21] Andrew Y. *et al* 2006 *Plasma Phys. Control. Fusion* **48** 479
[22] Sauter P. *et al* 2012 *Nucl. Fusion* **52** 012001
[23] Hubbard A.E. *et al* 1998 *Plasma Phys. Control. Fusion* **40** 689
[24] Fukuda T. *et al* 2000 *Plasma Phys. Control. Fusion* **42** A289
[25] Ryter F. *et al* 1996 *Nucl. Fusion* **36** 1217